# A Theoretical Study of BN-Confined Graphene Nanoribbon Based Resonant Tunneling Diodes

H. Nematian[1], M. Moradinasab[2,3], M. Noei[3], M. Pourfath[3,2], M. Fathipour[3], and H. Kosina[2]
[1]Department of Electronics, Science and Research Branch, Islamic Azad University, Tehran, Iran
[2]Institute for Microelectronics, TU Wien, Gußhausstraße 27–29/E360, 1040 Wien, Austria
[3]School of Electrical and Computer Engineering, University of Tehran, Tehran, Iran

e-mail: h.nematian@ieee.org

The negative differential resistance (NDR) of resonant tunneling diodes (RTDs) enables their use in fast-switching applications and logic circuit designs. So far, RTDs have been realized in Si/SiGe or III-V compound material systems. However, various emerging devices have been proposed and studied in the past two decades. Recently, graphene nanoribbons (GNRs) have attracted much attention as the potential building blocks of future electronics. Their exciting electrical properties such as high carrier mobility [1] and width-dependent bandgap [2], as well as their compatibility with the currently employed planar technology suggest that GNRs can be used as high performance RTDs [3]. In this work, we compare the I-V characteristics of the previously studied Hydrogen (H) passivated GNR RTDs with that of a Boron Nitride (BN) confined GNR RTDs for the first time. Our results indicate that BN-GNR RTDs demonstrate a higher peak-to-valley current ratio (PVCR) compared to H-GNR RTDs.

We employed the non-equilibrium Greens function (NEGF) formalism along with a second nearest neighbor tight-binding model [4] to describe the electronic bandstructure. In order to resolve the narrow resonance peaks with a resonable number of energy grid points an adaptive algorithm has been used [5].

We have performed simulations on different device geometries (represented by $S$, $H$, and $W$), see Fig. 1. The transmission probabilities as well as the current-voltage characteristics of H-GNR RTDs are shown in Fig. 2 and Fig. 3, respectively. Although the channel length and width of these three structures are similar, but they demonstrate different PVCRs. The $W$-shaped device exhibits a PVCR of 5 which is the smallest among the three types. This behavior is explained by a better path for the off-current provided in this channel geometry resulting in a higher valley current [3]. The other device shapes S and H have PVCRs of about 11, which renders them more suited for RTD applications.

Fig. 4 shows the structure of BN-GNR RTDs that have been studied in our work. The transmission probability and the current voltage characteristics of theses structures are shown in Fig. 5 and Fig. 6, respectively. The results indicate that BN-con fined devices outperform the H-passivated devices in terms of PVCR by at least one order of magnitude. The sharp resonant transmission peaks (see Fig. 5) result in PVCRs of about 90 for H-shaped, 300 for W-shaped, and 1200 for S-shaped RTDs for the first current peak, and PVCRs of about 18 for H-shaped, 42 for W-shaped, and 27 for S-shaped RTDs is achieved for the second current peak. BN-con fined GNR RTDs demonstrate acceptable PVCRs even when the nanoribbon indices are $3p + 2$. Previous works on H-passivated GNR RTDs have not studied these subfamilies due to their semi-metallic nature. The large ionic potential difference between B and N atoms near the GNR edges causes a considerable bandgap opening in the $3p + 2$ GNRs, making them suitable for RTDs. The results indicate that BN-confined GNRs are better candidates for RTD applications compared to H-passivated GNRs.

## Acknowledgment

This work, as part of the ESF EUROCORES program EuroGRAPHENE, is partly supported by funds from FWF, contract I420-N16.

## References

[1] A. Geim *et al.*, Nature Mater. **6**, 183 (2007).
[2] Z. Xu *et al.*, Appl. Phys. Lett. **90**, 223115 (3pp) (2007).
[3] H. Teong *et al.*, **105**, 084317 (6pp) (2009).
[4] G. Seol *et al.*, Appl. Phys. Lett. **98**, 143107 (3pp) (2011).
[5] M. Pourfath *et al.*, J. Comp. Electronics **5**, 155 (2006).

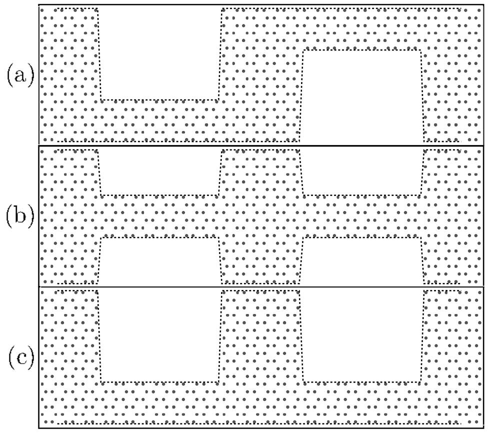


Fig. 1. Different geometrical structures of H-AGNR RTDs denoted by (a) $S$, (b) $H$, and (c) $W$, respectively.

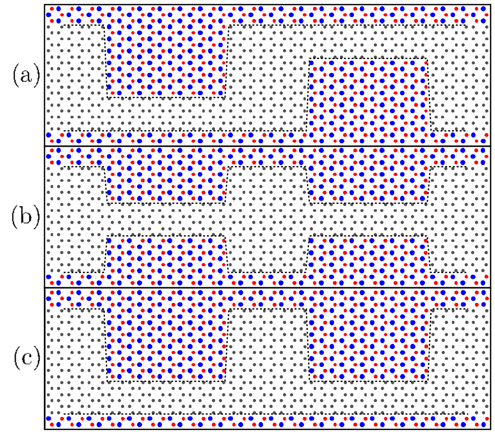


Fig. 4. Different geometrical structures of BN-AGNR RTDs denoted by (a) $S$, (b) $H$, and (c) $W$, respectively.

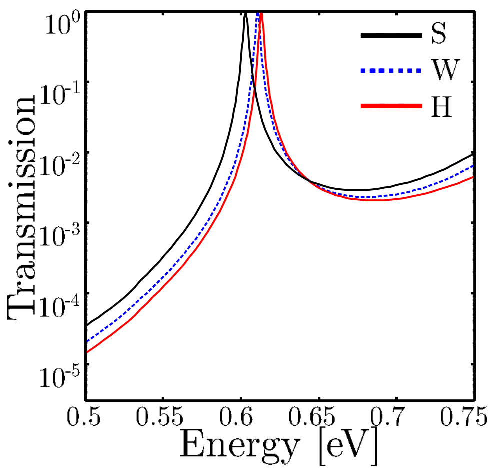


Fig. 2. Transmission probability as function of energy for H-AGNR RTDs.

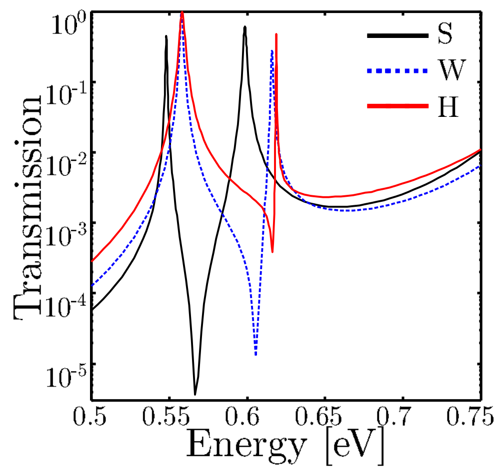


Fig. 5. Transmission probability as function of energy for BN-AGNR RTDs.

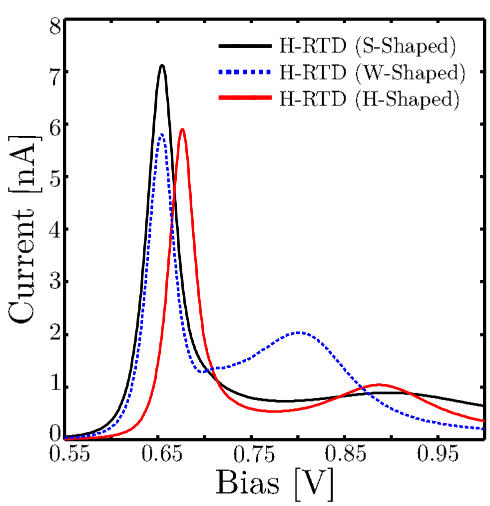


Fig. 3. Current-voltage characteristics of H-AGNR RTDs.

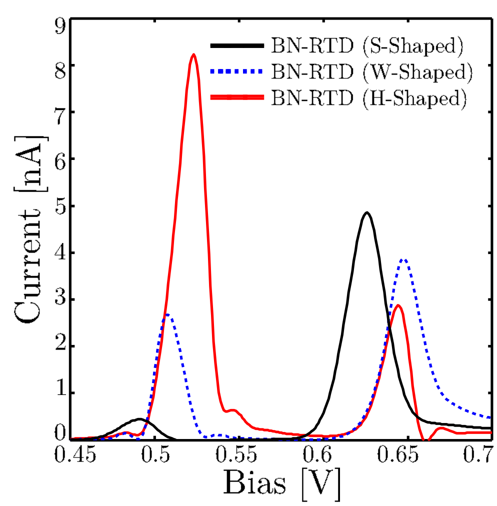


Fig. 6. Current-voltage characteristics of BN-AGNR RTDs.